

# Hsa\_Circular RNA\_0001013 Exerts Oncogenic Effects in Gastric Cancer Via the microRNA-136/TWSG1 Axis

**Zhaofeng Gao**

Zhejiang Chinese Medical University

**Lingyu Hu**

The Second Affiliated Hospital of Jiaxing University

**Fei Chen**

The Second Affiliated Hospital of Jiaxing University

**Chunhua He**

The Second Affiliated Hospital of Jiaxing University

**Biwen Hu**

The Second Affiliated Hospital of Jiaxing University

**Xiaoguang Wang** (✉ [xiaoguangwangs@163.com](mailto:xiaoguangwangs@163.com))

Zhejiang Chinese Medical University

---

## Research Article

**Keywords:** Gastric cancer, Circ\_0001013, miR-136, TWSG1, Migration, Invasion, Apoptosis

**Posted Date:** January 3rd, 2022

**DOI:** <https://doi.org/10.21203/rs.3.rs-1012547/v2>

**License:** © ⓘ This work is licensed under a Creative Commons Attribution 4.0 International License.

[Read Full License](#)

---

# Abstract

**Background** Gastric cancer (GC) is one of the most principle malignant cancers in the digestive system. Moreover, the critical role of circular RNAs (circRNAs) has been identified in GC development.

**Methods** In this context, the purpose of research was to explore the regulatory mechanism circ\_0001013, a novel circRNAs predicted by our research, in GC. The differential circRNAs and related mechanism in GC were predicted by microarray analysis. Circ\_0001013, miR-136, and TWSG1 expression in GC clinical samples and cells was detected by RT-qPCR. The relationship among circ\_0001013, miR-136, and TWSG1 was assessed by dual-luciferase reporter assay, biotin coupled probe pull-down assay, and biotin coupled miRNA capture. After gain- and loss-of-function assays in GC cells, cell proliferation, migration, invasion, and cell cycle and apoptosis were measured by EdU assay, scratch test, Transwell assay, and flow cytometry respectively. The effect of circ\_0001013 on tumor growth was detected by xenograft tumor in nude mice.

**Results** Microarray analysis predicted a novel circRNA, circ\_0001013, was upregulated in GC, which was confirmed by RT-qPCR detection in GC tissues and cells. Besides, miR-136 was downregulated but TWSG1 was highly expressed in GC tissues. Mechanically, circ\_0001013 could bind to miR-136, and miR-136 negatively targeted TWSG1 in GC cells. Silencing circ\_0001013 or TWSG1 or overexpressing miR-136 decreased GC cell proliferation, migration, invasion, and cell cycle arrest and accelerated cell apoptosis. Circ\_0001013 silencing decreased TWSG1 expression and inhibited transplanted tumor growth in nude mice.

**Conclusion** Circ\_0001013 elevated TWSG1 expression by binding to miR-136, thereby exerting oncogenic effect in GC.

## Introduction

As a heterogeneous disease and the end point of a long and multistep process, GC is caused by the gradual accumulation of various (epi)genetic alterations, which triggers imbalance of oncogenic and anti-oncogenic pathways [1]. As reported, gastric cancer (GC) ranks as fifth regarding to its morbidity and as third in cancer-related deaths, with over 1 million new cases and 784000 deaths globally in 2018) on a global scale [2]. There are risk factors for GC including diets low in fruit and vegetables, *Helicobacter pylori* infection, high salt intake, and age [3]. The presented symptoms of GC may include nausea, early satiety, emesis, anorexia, weight loss, dyspepsia, and epigastric pain, which are vague, non-specific, and may not occur until late in disease progression [4]. Unfortunately, although the development of biologic agents for GC has been advanced in the last decade, the prognosis of advanced GC remains extremely poor [5]. Thus, there is ongoing need to explore and understand the mechanism of action underlying GC for more accurate therapy for GC.

It is widely recognized that noncoding RNAs (ncRNAs), like circular RNAs (circRNAs), microRNAs (miRNAs, miRs), and long noncoding RNAs, assume crucial roles in GC development [6]. Moreover, the

oncogenic role of circRNAs has been identified in GC development via circRNA-miRNA-mRNA network [7]. For instance, circular RNA circLMO7 could induce GC progression by increasing the proliferation, invasion and migration capacities of GC cells via miR-30a-3p/WNT2 axis [8]. Hsa\_circ\_0001829 was capable of accelerating GC cell proliferation, migration and invasion, and decreasing cell cycle entry and apoptosis via miR-155-5p/SMAD2 axis [9]. Hsa\_circ\_0023409 regulated GC cell proliferation and metastasis via miR-542-3p/IRS4 axis [10]. More importantly, bioinformatics analysis of our study predicted the involvement of hsa\_circ\_0001013 in the pathogenesis of gastric cancer, and then we next further studied the downstream miRNA-mRNA mechanism of hsa\_circ\_0001013 in gastric cancer. Moreover, it was reported that miR-136 overexpression resulted in apoptosis in human GC cells [11]. However, the interaction between hsa\_circ\_0001013 and miR-136 was scarcely investigated. Besides, Twisted gastrulation BMP signaling modulator 1 (TWSG1) has been detected as an oncogene in papillary thyroid cancer (PTC) [12]. However, it is undefined about the interaction between miR-136 and TWSG1 in GC development. Therefore, tissue, cell, and animal experiments were implemented in our research to figure out whether there was hsa\_circ\_0001013-miR-136-TWSG1 network to affect GC development.

## Materials And Methods

### Ethical audit certificates

The human experiment was approved by the ethics committee of The Second Affiliated Hospital of Jiaying University and complied with the human medical research ethics in *Declaration of Helsinki*. All subjects signed an informed consent form before registration. The animal experiment procedures were carried out in accordance with the ethical standards of the animal experiment system approved by the Animal Ethics Committee of the Second Affiliated Hospital of Jiaying University. All measures were taken to minimize the pain of the included animals.

### Bioinformatics analysis

Microarray data GSE83521 of GC-related circRNAs was obtained from Gene Expression Omnibus database. The affy package in R software [13] was adopted for pre-processing and normalization of The microarray data. The limma package [14] was utilized to screen differential circRNAs with  $\log_2FC > 1$  or  $< -1$  and  $p < 0.05$  as the criteria, followed by drawing of heat map of the differential circRNAs. The possible regulatory mechanism of circ\_0001013 was further predicted by circinteractome database. The target genes of miR-136 were analyzed by miRDB (<http://www.mirdb.org/>), StarBase (<http://starbase.sysu.edu.cn/>), microT ([http://diana.imis.athena-innovation.gr/DianaTools/index.php?r=microT\\_CDS/](http://diana.imis.athena-innovation.gr/DianaTools/index.php?r=microT_CDS/)), and mirDIP (<http://ophid.utoronto.ca/mirDIP/>). Differentially expressed gene analysis was performed based on GC samples of TCGA database via GEPIA tool. The jvenn web tool (<http://jvenn.toulouse.inra.fr/app/example.html>) was utilized to obtain the intersection of analyzed miRNA-target genes and differentially highly expressed genes in GC. The survival curve was analyzed through KMplot tool (<http://kmplot.com/>).

### Construction of vector and detection of circ\_0001013 target gene by dual-luciferase reporter assay

The target gene of circ\_0001013 was predicted by circinteractome database, and dual-luciferase reporter assay was implemented to investigate whether miR-136 was a direct target gene of circ\_0001013. The sequences were obtained in GenBank database (National Center for Biotechnology Information, Bethesda, MD, USA). According to the prediction results, the sequences 3'-untranslated region (UTR) of miR-136 (potential target gene of circ\_0001013) was designed. One-step Site-directed Mutagenesis was employed to clone reporter gene plasmid vectors containing miR-136-3'UTR wild type and miR-136-3'UTR mutant type. Overexpression (oe)-circ\_0001013 was co-transfected with miR-136-Wt or miR-136-Mut plasmids into cells for 24 hours. After 6 hours of conventional culture in 5% CO<sub>2</sub> incubator at 37°C, the new medium was replaced. After 48 hours of continuous culture, the cells were lysed. The 100 µL PLB was added to each well, shaken at low speed for 15 minutes, and set aside at -4°C. Dual-luciferase reporter assay was operated as per the manuals of a dual luciferase reporter gene assay kit (#E1910) from Hangseng Biotechnological Company (Inner Mongolia, China): 100 µL fluorescein assay reagent II was taken in the 1.5 mL EP tube, and a TD20/20 Luminometer (Turner Designs, Sunnyvale, CA) was initiated to predict for 2 seconds. The tube was supplemented with 20 µL cell lysis, mixed completely, and positioned in the Luminometer to determine Firely Luciferase (FLUC). Then the 100 µL Stop&Glo preparation was added to measure Rellia Luciferase (RLUC). The relative luciferase intensity was calculated by RLUC/FLUC. According to RLUC/FLUC, the target sites of miRNA were determined.

### **Detection of dual luciferase activity**

The target genes of miR-136 were analyzed by biological prediction website ([http://www.targetscan.org/vert\\_72/](http://www.targetscan.org/vert_72/)). TWSG1 was confirmed to be the direct target of miR-136 via dual-luciferase reporter assay. The TWSG1 3'UTR gene fragment was cloned into pMIR-reporter. The sequenced luciferase reporter plasmids Wt and Mut were co-transfected with miR-136 into HEK-293T cells respectively. The cells were lysed after transfection for 48 hours. The luciferase activity was estimated by a Dual-Luciferase Reporter Assay System (Promega).

### **Sample collection**

Collected gastric cancer and para-carcinoma tissue from patients who were diagnosed with gastric cancer in the Second Affiliated Hospital of Jiaying University and received surgical treatment from 2016 to 2019. All patients had not received drug treatment before. A total of 70 pairs of tissue samples were immediately frozen in liquid nitrogen at -80°C.

### **Cell transfection**

Human 293T cells and human normal gastric epithelial cells RGM-1 were cultured in DMEM (Thermo Fisher Scientific Inc., Waltham, MA, USA). Human GC cell lines MGC-803, SGC-790, MKN45 and HGC-27 were cultured in RPMI 1640 medium. All above medium were supplemented with 10% fetal bovine serum (Gibco, Carlsbad, California, USA), 100 U/mL penicillin, and 100 mg/mL streptomycin. All cells were cultured in a incubator with saturated humidity and 5% CO<sub>2</sub> at 37°C.

## Reverse transcription quantitative polymerase chain reaction (RT-qPCR)

Total RNA was extracted by Trizol. The concentration and purity of RNA were determined via spectrophotometry, the RNA integrity was assessed by agarose gel electrophoresis. miRNA specific complementary DNA was synthesized by a TaqMan MicroRNA reverse transcription kit and the primers from TaqMan MicroRNA Assay. miR-136 expression was measured in the light of the protocols of TaqMan miRNA Assays and standardized by U6. The primers were synthesized by Beijing Genomics Institute (BGI, Beijing, China) (Table 1). The reverse transcription experiment was taken by the directions of EasyScript First-Strand cDNA Synthesis SuperMix (AE301-02, Beijing TransGen Biotech Co., Ltd.). The reaction solution was taken for real-time fluorescent quantitative PCR on a real-time fluorescent quantitative PCR instrument (ABI 7500, ABI, Foster City, CA, USA) in accordance with the instructions of SYBR®Premix Ex Taq™ II kit (Takara, Dalian, China). The  $2^{-\Delta\Delta Ct}$  was the relative quantitative expression target gene expression.

## Western blot

Cells were lysed with RIPA cell lysis buffer (P0013B, Beyotime, Shanghai, China) encompassing phenylmethylsulfonyl fluoride at the final concentration of 1 mM. The protein was quantified by a Bio-Rad DC Protein Assay kit (EWELL Bio-Technology Co., Ltd., Guangdong, China). Each sample was mixed with sodium dodecyl sulfate buffer and boiled for 10 minutes. The samples were subjected to gel electrophoresis at 80 V for 30 min and 120 V for 90 min. The proteins were electrically imprinted from the gel onto a PVDF membrane at a constant current of 300 mA for 90 min. The membrane was blocked with tris-buffered saline with Tween 20 containing 5% skimmed milk powder and shaken at 37 degrees Celsius for 2 hours. The membrane was probed with primary antibodies (Abcam, Cambridge, UK) to TWSG1 (ab218995, mouse, 1:1000) and glyceraldehyde-3-phosphate dehydrogenase (GAPDH) (ab8245, mouse-anti-human, 1:5000) at 4°C for 12h, followed by 1-hour re-probing with goat anti-rabbit Immunoglobulin G (ab6721, 1:20000, Abcam) secondary antibody. Next, the sensitized electrogenerated chemiluminescence was applied for development of the blots. The gray value of protein bands was measured by an Image J software (NIH free software, USA).

## Scratch test

The cells were cultured in a 6-well plate with  $2.5 \times 10^4$  cells/cm<sup>2</sup>. After 24 hours, the medium was sucked off, and a 10  $\mu$ L sterilized disposable pipette was utilized to make a wound. The cells were washed twice with PBS and then cultured in RPMI 1640 medium containing 10% FBS. The wound healing of cells at 0 hour and 48 hour was observed at the same location. Each group is provided with three auxiliary holes. The migration ability of GC cells was expressed by Migration rate = (scratch width at T<sub>48</sub> - scratch width at T<sub>0</sub>) / scratch width at T<sub>0</sub> × 100%.

## Transwell assay

The apical chamber of Transwell (8  $\mu\text{m}$  aperture, Costar, Cambridge, Massachusetts, USA) was coated with Matrigel (BD Biosciences, Franklin Lakes, NJ, USA). Transfected cells ( $1 \times 10^4$  in 200  $\mu\text{L}$  serum-free medium) were seeded into the upper chamber for invasion detection. The medium encompassing 10% FBS was added to the bottom chamber as a chemical attractant. Cells were incubated at 37  $^\circ\text{C}$  for 48 hours to detect invasion in a 5%  $\text{CO}_2$  chamber. After incubation, the cells in the apical chamber were removed by cotton swabs, and on the lower surface were fixed with methanol, stained with 0.1% crystal violet and observed under a microscope (200 $\times$ , Olympus, Tokyo, Japan).

### **Flow cytometry**

Total  $1 \times 10^6$  cells in logarithmic phase were fixed with 70% cold ethanol, mixed with 1 mL propidium iodide staining solution (Becton Dickinson, Franklin Lakes, NJ, USA, 50  $\mu\text{g}/\text{mL}$ ), and then placed in dark for 30 minutes. Cell cycle was determined by a FACS Calibur flow cytometer. The above results were analyzed with professional software ModFit.

Total  $1 \times 10^6$  cells in logarithmic phase in  $1 \times$  Annexin buffer. Cells were double stained with 5  $\mu\text{L}$  Annexin-V<sup>FITC</sup> (Becton Dickinson) and 1  $\mu\text{L}$  PI in dark for 10 minutes. The mixture was placed in dark for 5 minutes. Cells were suspended with 300  $\mu\text{L}$  of  $1 \times$  Annexin buffer. The result was analyzed with flow cytometry.

### **EdU assay**

GC cells in the NC group and the short hairpin RNA (si)-hsa\_circ\_0001013 group were labeled with EdU. The method was implemented as per the protocols of EdU proliferation detection kit (CA1170, Solarbio, Beijing, China). After removing the supernatant, 100  $\mu\text{L}$  medium containing EdU (30  $\mu\text{mol}/\text{L}$ ) was added to each well for 12-hour cell incubation. After discarding the medium, cells were fixed with 4% paraformaldehyde for half an hour. After discarding the fixative solution, the cells were mixed with 50  $\mu\text{L}$  of 2 mg/mL glycine for 5 minutes. Then 100  $\mu\text{L}$  Apollo<sup>®</sup> staining solution was added into cells in dark treatment, followed by nuclear staining with Hoechst33342 (Thermo Fisher Scientific Inc.). ImagePro software was applied for image acquisition and quantitative analysis.

### **Biotin coupled probe pull-down assay**

The biotinylated probe sequence of hsa\_circ\_0001013 was 5'-FITC- GGACCGAGTCAAGTCAAAGG -3'. About  $1 \times 10^7$  cells were lysed in lysis buffer and placed with 3  $\mu\text{g}$  biotinylated probe for 2 hours at room temperature. Cell lysates were cultured with streptavidin magnetic beads (Life Technology, Gaithersburg, MD, USA) for 4 hours to pull down the biotin coupled RNA complex. The magnetic beads were washed five times with lysis buffer. The miRNA in complex was extracted with Trizol reagent to used to do real-time quantitative PCR.

### **Biotin coupled miRNA capture**

About  $2 \times 10^6$  cells were lysed with 50  $\mu$ m biotinylated miRNA mimics at 50% aggregation state, and the sequence was GCCCTTCATGCTGCCAG. After transfection for 24 hours, the cells were lysed in lysis buffer. Mixed 50  $\mu$ L streptavidin beads for 2 h, then added to tubes and pulled down biotin-conjugated RNA complex. The tubes were incubated at low speed (10 r/min) for 4 hours on a rotator. After that the beads were washed several times with lysis buffer, RNA specifically interacting with miRNA was recovered with Trizol LS (Life Technology). The abundance of hsa\_circ\_0001013 was assessed by RT-qPCR and agarose gel electrophoresis.

### **Northern blot analysis**

The analysis was performed with a Northern blot Kit (Ambion, Company, Austin, TX, USA). In a word, the total RNA was denatured in formaldehyde and electrophoresed in 1% agarose-formaldehyde gel. Then the RNA was transferred to Hybond-N + nylon membrane and hybridized with biotin-labeled DNA probe. Binding RNA was detected using a biotin chromogenic assay kit. Finally, the membrane was analyzed by an Image Lab software (Bio-Rad, Hercules, CA, USA).

### **Fluorescence In Situ Hybridization**

The hsa\_circ\_0001013 sequence and miR-136 specific probe were adopted for FISH. In short, a cy5-labeled and farm-labeled probe was specifically targeted cirC\_0001013 and miRNA, respectively. The nuclei were stained by 4',6-Diamidino-2-Phenylindole. All steps were performed according to the manufacturer's instructions. The image was obtained on a Zeiss LSM880 NLO confocal microscope system (Leica Microsystems, Mannheim, GER).

### **Mouse xenografts**

MGC-803 cells ( $1 \times 10^7$ ) were subcutaneously injected into the left armpit of BALB/C nude mice (aged 4-6 weeks, weighing 18 g-22 g, 8 mice/group) to establish xenograft mouse model. After the tumor volume grew to 100 mm<sup>3</sup>, si-circ\_0001013 alone, miR-136 alone or both were injected into the tumors of mice every two days for two weeks. The tumor volume was measured every other day according to the formula  $V = (W^2 \times L)/2$ . All mice were euthanized by CO<sub>2</sub> and weighed.

### **Immunohistochemistry**

The specimens were fixed with 10% formaldehyde and embedded in paraffin, and successively cut into 4  $\mu$ m slices. The slices were dried and dewaxed with xylene, then dehydrated with alcohol. The sections were immersed in 3% methanol H<sub>2</sub>O<sub>2</sub> for half an hour at 37°C. The sections were put into 0.01 M citrate buffer and boiled at 95°C for 20 minutes, and cooled to room temperature. Normal goat serum blocking solution was dripped onto the sections for 10-minute incubation at 37°C. The sections were incubated with primary antibodies to TWSG1 (ab57552, rabbit anti-human, 1:200), Ki-67 (ab156956, mouse, 1:150), matrix metalloproteinase 9 (MMP9, ab38898, rabbit, 1:500) and CD34 (ab81289, rabbit, 1:2500) at 4°C overnight. Afterwards, the corresponding biotin-labeled goat anti-rabbit secondary antibody was

added for 10-minute incubation at room temperature. The slices were incubated in Streptomyces ovalbumin working solution labeled with horseradish peroxidase (S-A/HRP) for 10 min at room temperature. After that, the slices were stained with diaminobenzidine for 8 minutes in a dark room at room temperature. Then the hematoxylin stained sections were dehydrated, cleared, sealed and observed under an optical microscope. A Nikon image analysis software from Japan was employed to count the positive cells. The number of positive cells was calculated in 3 equal area non-repeated fields in each section (200×). Criteria for judging immunohistochemical staining results: ABCF2 (positive staining was more than 25% of the cells), and obvious brown or brownish yellow granules appeared in the cytoplasm.

## Statistical analysis

SPSS 26.0 (IBM Corp. Armonk, NY, USA) was adopted for statistical analysis.  $P < 0.05$  indicated statistically significant difference. The measurement data were summarized as mean  $\pm$  standard deviation. The *T*-test was used to compare the experimental groups. One-way analysis of variance (ANOVA) was applied for comparison among multiple groups, while repeated measurement ANOVA was used to analyze the data at different time points, followed by Tukey's post-hoc test. Pearson correlation was conducted to analyze the relationship between the two indexes. Kaplan-Meier method was utilized to analyze the survival rate. Log-rank test was performed for univariate analysis.

## Results

### Circ\_0001013 was highly expressed in GC and correlated with prognosis

Initially, we explored the mechanism of circ\_0001013 in GC. Firstly, differentially expressed circRNAs in GC were screened by R language, and we found that circ\_0001013 was highly expressed in GSE83521 (Fig. 1A) and circ\_0001013 had the highest differential expression value ( $\log_2FC = 1.961257597$ ,  $p$  value = 0.000414929). Then, RT-qPCR in 70 pairs of GC tissues and matched adjacent normal tissues showed that hsa\_circ\_0001013 expression in GC tissues was notably higher than that in adjacent normal tissues (Fig. 1B). Patients were arranged into patients with high expression and patients with low expression with the median value as the boundary. According to the Kaplan-Meier survival curve (Fig. 1C), the survival rate of patients with high expression of circ\_0001013 was low, while the survival rate of patients with low expression of circ\_0001013 was markedly increased. In addition, hsa\_circ\_0001013 expression was higher in four GC cell lines (MGC-803, SGC-7901, MKN45 and HGC-27) compared with normal gastric epithelial cell line RGM-1 (Fig. 1D). Therefore, circ\_0001013 was upregulated in GC tissues and cells.

### Low expression of circ\_0001013 promoted cell cycle arrest and apoptosis while repressing cell proliferation, migration, and invasion of GC cells

In view of the high hsa\_circ\_0001013 expression in GC tissues and cell lines, we further investigated its potential function by silencing hsa\_circ\_0001013 in GC cell line HGC-27. FISH assay showed that circRNA was located in cytoplasm (Fig. 2A). RT-qPCR results indicated that the relative expression of hsa\_circ\_0001013 in the si-hsa\_circ\_0001013 group was significantly lower than that in the control group,

but there was no significant difference in the relative expression of linear 0001013 (Fig. 2B-C). Flow cytometry analysis showed that si-hsa\_circ\_0001013 induced G1-phase arrest (Fig. 2D) and apoptosis in GC HGC-27 cells (Fig. 2E). Colony formation assay displayed that the number of colonies in the si-hsa\_circ\_0001013 group was significantly lower than that in the NC group (Fig. 2F). CCK-8 assay and 5-ethynyl-2'-deoxyuridine (EdU) assay exhibited that the proliferation ability of GC cells in the si-hsa\_circ\_0001013 group was evidently lower than that in NC group (Fig. 2G-H). Cell scratch test and Transwell test also indicated that the migration and invasion of GC cells were obviously inhibited by si-hsa\_circ\_0001013 (Fig. 2I-J). Collectively, circ\_0001013 downregulation decreased cell proliferation, migration, and invasion but enhanced cell cycle arrest and apoptosis in GC.

### **Circ\_0001013 bound to miR-136 to downregulate it in GC cells**

Bioinformatics analysis (Starbase V2.0, Circinteractome) showed that hsa\_circ\_0001013 might bind to miR-136 in GC cells (Fig. 3A). Pull down test and RT-qPCR analysis displayed that miR-136 was obviously pulled down by the circRNA probe. Moreover, Wt miR-136 captured more circRNA in HGC-27 cells overexpressing circRNA using biotin-labeled miR-136 and its mutant mimics (Fig. 3B-D). Luciferase reporter gene experiment showed that miR-136 mimic strikingly reduced the luciferase activity of complete circRNA sequence, but did not affect the luciferase activity with miR-136-Mut (Fig. 3E). Based on FISH results, circRNA and miR-136 were co-located in the cytoplasm (Fig. 3F). It was found that the expression of miR-136 was low in GC tissues (Fig. 3G). Correlation analysis demonstrated that hsa\_circ\_0001013 was negatively correlated with miR-136 in GC tissues (Fig. 3H). It was found that miR-136 decreased with the overexpression of circ\_0001013 and increased with silencing of circ\_0001013 in MGC-803 cells (Fig. 3I), indicating that circ\_0001013 could bound to miR-136 in GC cells.

### **miR-136 eliminated the cancer promoting effect of hsa\_circ\_0001013 on GC**

Then we evaluated the potential function of miR-136 in GC by co-transfecting MGC-803 cells with miR-136 mimic and circ\_0001013 plasmids. Cell migration was detected by scratch test, cell invasion by Transwell, and cell cycle and apoptosis by flow cytometry. The results documented that cell migration, in the hsa\_circ\_0001013 overexpression augmented cell migration (Fig. 4A), invasion (Fig. 4B), and the number of cells at G2 phase (Fig. 4C) and diminished cell apoptosis (Fig. 4D) of MGC-803 cells, which was normalized by further miR-136 mimic. Conclusively, the oncogenic effect of hsa\_circ\_0001013 on GC was abolished by miR-136 overexpression.

### **circ\_0001013 upregulated the target gene TWSG1 of miR-136**

A total of 225, 2649, 434 and 187 potential target genes of miR-136 were predicted by miRDB, StarBase, microT, and mirDIP, respectively. Then, 3741 genes were significantly highly expressed in GC predicted by the GEPIA tool, and 12 candidate genes were obtained by taking the intersection of predicted target genes and differentially highly expressed genes in GC (HOXC10, CBX4, ZNF710, CAMSAP2, MTPN, ZNF148, XIAP, ANXA4, MBNL3, DCAF7, TNRC18, and TWSG1) (Fig. 5A). The GEPIA tool and KMplo tool finally found that TWSG1 was highly expressed in GC and followed up with the prognosis of GC (Fig. 5B, C).

StarBase showed that miR-136 had a binding site with TWSG1 in GC cells (Fig. 5D). Dual-luciferase reporter assay proved that miR-136 mimic strongly decreased luciferase activity of TWSG1-Wt, while TWSG1-Mut had no significant difference (Fig. 5E). Then, RT-qPCR exhibited that TWSG1 expression in GC tissues was remarkably higher than that in adjacent normal tissues (Fig. 5F). Correlation analysis demonstrated that there was a positive correlation between the expression of hsa\_circ\_0001013 and TWSG1 (Fig. 5G). In order to detect whether hsa\_circ\_0001013 can regulate the target gene TWSG1 to exert its anti-tumor effect by miR-136, RT-qPCR and western blot analysis results exhibited that overexpression of hsa\_circ\_0001013 could enhance the mRNA and protein levels of TWSG1 (Fig. 5H-I), while miR-136 mimic transfection evidently diminished the mRNA and protein levels of TWSG1 (Fig. 5J-K). All the above results certificated that TWSG1 was a direct target of miR-136. The co-transfection of hsa\_circ\_0001013 and miR-136 mimic was utilized for further evaluating the expression of TWSG1. It was found that overexpression of hsa\_circ\_0001013 could partially rescue the inhibition of miR-136 on TWSG1 expression (Fig. 5L). In summary, hsa\_circ\_0001013 bound to miR-136 to upregulate TWSG1 in GC cells.

### **Low expression of circ\_0001013 inhibited xenograft tumorigenesis in nude mice**

Then, we investigated whether the overexpression of hsa\_circ\_0001013 affected tumor growth in vivo. The mice model of xenotransplantation was established by subcutaneous injection of equal amount of MGC-803 cells (n = 8 in each group). After about 10 days, when the tumor volume reached about 100 mm<sup>3</sup>, the constructed plasmids were injected into the tumor every two days for two weeks to construct the si-hsa\_circ\_0001013 group, the oe-miR-136 group and the si-circ\_0001013 + oe-miR-136 group. The tumor volume and final weight were measured every other week. Compared with the NC group, the average tumor volume and weight of the oe-miR-136 group and the si-hsa\_circ\_0001013 group were obviously reduced (Fig. 6A-B), while the average tumor volume and weight of the si-circ\_0001013 + oe-miR group were most memorably declined in contrast to the si-hsa\_circ\_0001013 group. Western blot analysis displayed that the expression of TWSG1 protein was dramatically decreased in the oe-miR-136 group and the si-hsa\_circ\_0001013 group (Fig. 6C), while the expression of TWSG1, Ki-67, MMP9 and CD34 protein was most substantially lessened in the si-circ\_0001013 + oe-miR-136 group. Immunohistochemistry analysis showed that the abundances of TWSG1, Ki-67, MMP9 and CD34 were markedly decreased after silencing of hsa\_circ\_0001013 and overexpression of miR-136 (Fig. 6D). To sum up, hsa\_circ\_0001013 downregulation repressed xenograft tumorigenesis in nude mice.

## **Discussion**

In spite of the declining incidence and mortality, GC is still one of the most principle cancers across the world [15]. In addition, GC diagnosis and prognosis are still poor because GC patients are usually diagnosed at an advanced stage [16]. Therefore, it is critical to study the molecular mechanism behind GC development for better understanding of GC. Therefore, we conducted this work to figure out the mechanism of hsa\_circ\_0001013/miR-136/TWSG1 axis in GC, and observed that hsa\_circ\_0001013

overexpression enhanced TWSG1 expression by binding to miR-136, which promoted the proliferation, migration, and invasion and inhibited the apoptosis of GC cells.

As widely recognized, a variety of circRNAs are involved in GC cell proliferation, apoptosis, migration, and invasion with aberrant expression [17]. For example, hsa-circ-0000670 expression was high in GC tissues and cell lines, and its upregulation could potentiate the proliferative, invasive and migrating capabilities of GC cells [18]. Also, circNRIP1 was overexpressed in GC tissues, and its silencing diminished GC cell proliferation, migration, and invasion [19]. Besides, hsa\_circ\_0000467 was upregulated in GC tissues and cell lines, and hsa\_circ\_0000467 downregulation caused depression of GC cell proliferation, invasion, and cell cycle entry [20]. Furthermore, circCACTIN upregulation was observed in GC tissues and cells, and its knockdown triggered inhibition of GC cell proliferation, migration, and invasion [21]. In line with these findings, microarray analysis predicted high circ\_0001013 expression in GC samples, which was verified by RT-qPCR detection of circ\_0001013 expression in GC tissues and cells. Notably, further cell function experiments indicated decline of GC cell proliferation, invasion, and migration but acceleration of cell apoptosis and cell cycle arrest after silencing hsa\_circ\_0001013, thus supporting the oncogenic role of hsa\_circ\_0001013 in GC development.

As reported, circRNAs can function as competing endogenous RNAs or miRNA sponges to bind to miRNAs through a miRNA response element, thus negatively orchestrating activity of miRNAs [22]. In line with this, it was uncovered in our research that hsa\_circ\_0001013 bound to miR-136 to downregulate miR-136 in GC cells. Additionally, we also found that miR-136 expression was poor in GC tissues, and that miR-136 overexpression in GC cells reduced cell cycle entry, proliferation, invasion, and migration while elevating cell apoptosis. Coincident with our results, a prior study manifested that miR-136 was poorly expressed in GC cells, and that enforced expression of miR-136 contributed to increase of GC cell apoptosis by targeting AEG-1 and BCL2 [11]. Consistently, another work discovered that miR-136 upregulation led to the repression of GC cell proliferation, migration, and invasion [23]. Also, it was noted in the research of Jin *et al.* that miR-136 was lowly expressed in colorectal cancer (CRC) tissues and cell lines, and that ectopically expressed miR-136 caused reduction of CRC cell proliferation, migration, and invasion and arresting of cell at G0/G1 phase [24]. Additionally, miR-136 downregulation was detected in endometrial cancer (EC) tissues and cells, and miR-136 upregulation decreased EC cell proliferation, migration, and invasion [25]. Collectively, these evidences supported the tumor suppressive capacities of miR-136 in GC development.

It is well-known that miRNAs can repress expression of target mRNAs by binding to their 3'-UTR, thus participating in the pathological processes of human diseases, like cancer [26]. Similarly, bioinformatics analysis, dual luciferase activity assay, and RT-qPCR of our study illustrated that miR-136 bound to 3'-UTR of TWSG1 to decrease TWSG1 expression in GC cells. Further analysis in our research elucidated that TWSG1 was upregulated in GC tissues, and that miR-136 overexpression led to decreased GC cell proliferation, invasion, and migration and enhanced cell cycle arrest and apoptosis by downregulating TWSG1. Consistently, PTC tissues contained upregulated TWSG1, and TWSG1 knockdown depressed migration, invasion and proliferation of PTC cells [12]. In addition, the research

conducted by Liu et al. elaborated that TWSG1 expression was substantially augmented in glioma tissues versus normal brain tissue, and that TWSG1 upregulation caused enhancement of glioma cell proliferation [27].

In conclusion, we identified a novel circRNA hsa\_circ\_0001013 that elevated the proliferation, migration, and invasion while diminishing apoptosis of GC cells through binding to miR-136 and positively regulating TWSG1 expression (Fig. 7). Our results revealed the critical roles of the hsa\_circ\_0001013/miR-136/TWSG1 axis in GC, which provided a new molecular target for the therapy of GC.

## **Declarations**

### **ACKNOWLEDGEMENTS**

Not applicable.

### **Ethics approval and consent to participate**

This study was approved by the Ethics Committee of the Second Affiliated Hospital of Jiaxing University.

### **Patient consent for publication**

Informed consent of each research participant was obtained.

### **FUNDING**

This work was supported by the science and technology planning project of Jiaxing City (No. 2017BY18014)

### **CONFLICTS OF INTEREST**

The authors declare no conflict of interest.

### **AUTHOR CONTRIBUTIONS**

Xiaoguang Wang and Biwen Hu participated in the conception and design of the study. Chunhua He and Fei Chen performed the analysis and interpretation of data. Zhaofeng Gao and Lingyu Hu contributed to drafting the article. Lingyu Hu and Xiaoguang Wang revised it critically for important intellectual content. All authors approved the final version of the manuscript.

### **AVAILABILITY OF DATA AND MATERIAL**

The datasets generated during the current study are available.

## **References**

1. S. Molina-Castro, J. Pereira-Marques, C. Figueiredo et al., "Gastric cancer: Basic aspects," *Helicobacter*, Vol. 22 Suppl 1, no. pp. 2017.
2. F. Bray, J. Ferlay, I. Soerjomataram et al., "Global cancer statistics 2018: GLOBOCAN estimates of incidence and mortality worldwide for 36 cancers in 185 countries," *CA Cancer J Clin*, Vol. 68, no. 6, pp. 394-424, 2018.
3. E. C. Smyth, M. Nilsson, H. I. Grabsch et al., "Gastric cancer," *Lancet*, Vol. 396, no. 10251, pp. 635-648, 2020.
4. F. M. Johnston, M. Beckman, "Updates on Management of Gastric Cancer," *Curr Oncol Rep*, Vol. 21, no. 8, pp. 67, 2019.
5. C. Coutzac, S. Pernot, N. Chaput et al., "Immunotherapy in advanced gastric cancer, is it the future?," *Crit Rev Oncol Hematol*, Vol. 133, no. pp. 25-32, 2019.
6. L. Wei, J. Sun, N. Zhang et al., "Noncoding RNAs in gastric cancer: implications for drug resistance," *Mol Cancer*, Vol. 19, no. 1, pp. 62, 2020.
7. J. Cheng, H. Zhuo, M. Xu et al., "Regulatory network of circRNA-miRNA-mRNA contributes to the histological classification and disease progression in gastric cancer," *J Transl Med*, Vol. 16, no. 1, pp. 216, 2018.
8. J. Cao, X. Zhang, P. Xu et al., "Circular RNA circLMO7 acts as a microRNA-30a-3p sponge to promote gastric cancer progression via the WNT2/beta-catenin pathway," *J Exp Clin Cancer Res*, Vol. 40, no. 1, pp. 6, 2021.
9. Q. Niu, Z. Dong, M. Liang et al., "Circular RNA hsa\_circ\_0001829 promotes gastric cancer progression through miR-155-5p/SMAD2 axis," *J Exp Clin Cancer Res*, Vol. 39, no. 1, pp. 280, 2020.
10. J. Li, Y. Yang, D. Xu et al., "hsa\_circ\_0023409 Accelerates Gastric Cancer Cell Growth and Metastasis Through Regulating the IRS4/PI3K/AKT Pathway," *Cell Transplant*, Vol. 30, no. pp. 963689720975390, 2021.
11. L. Yu, G. Q. Zhou, D. C. Li, "MiR-136 triggers apoptosis in human gastric cancer cells by targeting AEG-1 and BCL2," *Eur Rev Med Pharmacol Sci*, Vol. 22, no. 21, pp. 7251-7256, 2018.
12. S. Xia, R. Ji, Y. Xu et al., "Twisted Gastrulation BMP Signaling Modulator 1 Regulates Papillary Thyroid Cancer Cell Motility and Proliferation," *J Cancer*, Vol. 8, no. 14, pp. 2816-2827, 2017.
13. L. Gautier, L. Cope, B. M. Bolstad et al., "affy—analysis of Affymetrix GeneChip data at the probe level," *Bioinformatics*, Vol. 20, no. 3, pp. 307-315, 2004.
14. G. K. Smyth, "Linear models and empirical bayes methods for assessing differential expression in microarray experiments," *Stat Appl Genet Mol Biol*, Vol. 3, no. pp. Article3, 2004.
15. K. Lyons, L. C. Le, Y. T. Pham et al., "Gastric cancer: epidemiology, biology, and prevention: a mini review," *Eur J Cancer Prev*, Vol. 28, no. 5, pp. 397-412, 2019.
16. A. Sukri, A. Hanafiah, N. Mohamad Zin et al., "Epidemiology and role of Helicobacter pylori virulence factors in gastric cancer carcinogenesis," *APMIS*, Vol. 128, no. 2, pp. 150-161, 2020.

17. R. Li, J. Jiang, H. Shi et al., "CircRNA: a rising star in gastric cancer," *Cell Mol Life Sci*, Vol. 77, no. 9, pp. 1661-1680, 2020.
18. P. Liu, S. Cai, N. Li, "Circular RNA-hsa-circ-0000670 promotes gastric cancer progression through the microRNA-384/SIX4 axis," *Exp Cell Res*, Vol. 394, no. 2, pp. 112141, 2020.
19. X. Zhang, S. Wang, H. Wang et al., "Circular RNA circNRIP1 acts as a microRNA-149-5p sponge to promote gastric cancer progression via the AKT1/mTOR pathway," *Mol Cancer*, Vol. 18, no. 1, pp. 20, 2019.
20. W. L. Mo, J. T. Jiang, L. Zhang et al., "Circular RNA hsa\_circ\_0000467 Promotes the Development of Gastric Cancer by Competitively Binding to MicroRNA miR-326-3p," *Biomed Res Int*, Vol. 2020, no. pp. 4030826, 2020.
21. L. Zhang, X. Song, X. Chen et al., "Circular RNA CircCACTIN Promotes Gastric Cancer Progression by Sponging MiR-331-3p and Regulating TGFBR1 Expression," *Int J Biol Sci*, Vol. 15, no. 5, pp. 1091-1103, 2019.
22. L. Verduci, S. Strano, Y. Yarden et al., "The circRNA-microRNA code: emerging implications for cancer diagnosis and treatment," *Mol Oncol*, Vol. 13, no. 4, pp. 669-680, 2019.
23. X. Yu, W. Xiao, H. Song et al., "CircRNA\_100876 sponges miR-136 to promote proliferation and metastasis of gastric cancer by upregulating MIEN1 expression," *Gene*, Vol. 748, no. pp. 144678, 2020.
24. C. Jin, A. Wang, L. Liu et al., "Hsa\_circ\_0136666 promotes the proliferation and invasion of colorectal cancer through miR-136/SH2B1 axis," *J Cell Physiol*, Vol. 234, no. 5, pp. 7247-7256, 2019.
25. Y. Shi, L. Jia, H. Wen, "Circ\_0109046 Promotes the Progression of Endometrial Cancer via Regulating miR-136/HMGA2 Axis," *Cancer Manag Res*, Vol. 12, no. pp. 10993-11003, 2020.
26. Z. Ali Syeda, S. S. S. Langden, C. Munkhzul et al., "Regulatory Mechanism of MicroRNA Expression in Cancer," *Int J Mol Sci*, Vol. 21, no. 5, pp. 2020.
27. Z. Liu, H. Li, "Twisted gastrulation signaling modulator 1 promotes the ability of glioma cell through activating Akt pathway," *Neuroreport*, Vol. no. pp. 2021.

## Tables

**Table 1** The primers for RT-qPCR

Targets	Seuences (5'-3')
miR-136 F	ACUCCAUUUGUUUUGAUGAUGGA
miR-136 R	UCCAUCAUCAAAACAAAUGGAGU
U6 F	GCTTCGGCAGCACATATACTAAAAT
U6 R	CGCTTCACGAATTTGCGTGTCAT
circ_0001013 F	GGACCGAGTCAAGTCAAAGG
circ_0001013 R	GGAGGCTGAGGCAGAAGAAT
TWSG1 F	GCTGTGCTTACTCTAGCCATC
TWSG1 R	TGAGGCATTTGCTCACATCAC
GAPDH F	GGAGCGAGATCCCTCCAAAAT
GAPDH R	GGCTGTTGTCATACTTCTCATGG

## Figures

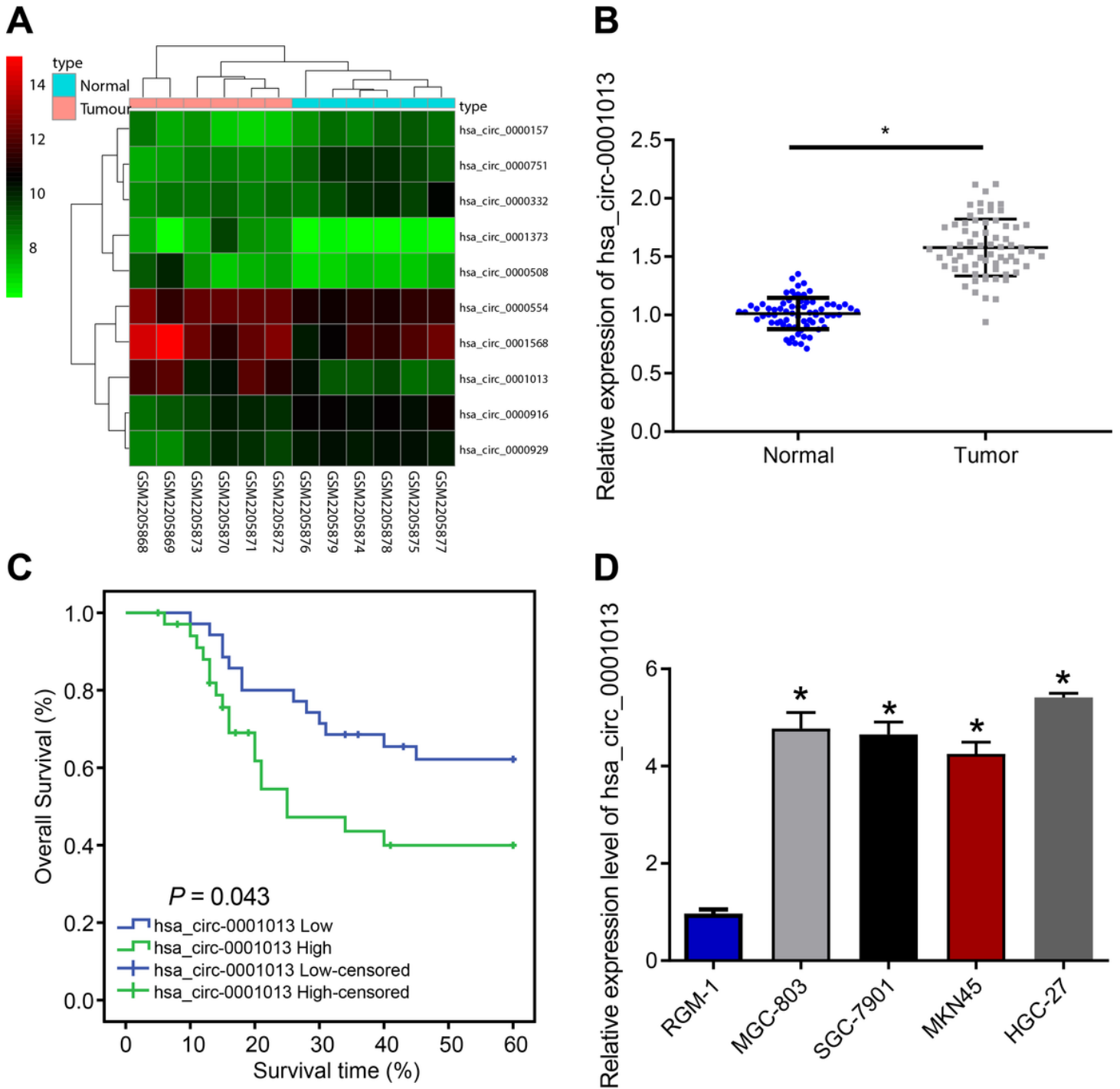


**Figure 1**

Upregulated circ\_0001013 is observed in GC tissues and cell, and associated with poor prognosis of GC patients. A, Heat map of the top 10 differentially expressed circRNAs in microarray data GSE83521. The abscissa represented the sample number, the ordinate expressed the differential gene, the upper right histogram was the color scale, and each rectangle in the graph corresponded to a sample expression value. B, RT-qPCR to detect the relative expression of hsa\_circ\_0001013 in GC and adjacent normal tissues (n = 70). C, Kaplan-Meier survival curve. D, RT-qPCR to measure the relative expression of

hsa\_circ\_0001013 in normal gastric epithelial cell line RGM-1 and four GC cell lines. \*  $p < 0.05$  vs. adjacent normal tissues and RGM-1 cells. The experiment was repeated three times.

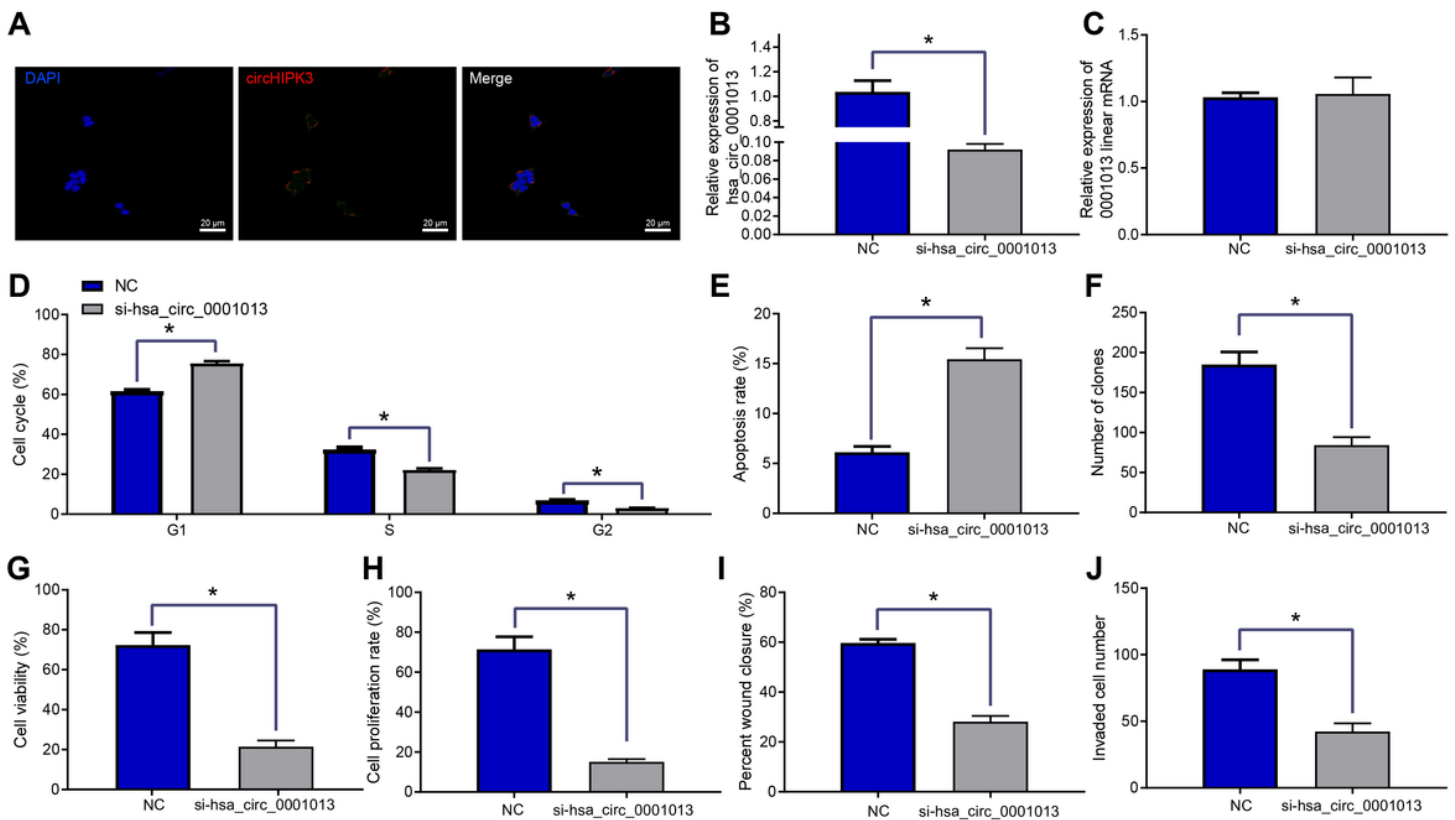


**Figure 2**

Low hsa\_circ\_0001013 expression induces cell cycle arrest and apoptosis and depresses cell proliferation, migration, and invasion of GC cells. A, FISH showed that circRNA was located in cytoplasm ( $\times 500$ ). GC cell line HGC-27 was transfected with si-hsa\_circ\_0001013 or NC. B, The relative expression of circ\_0001013 detected by RT-qPCR. C, RT-qPCR to determine the relative expression level of linear 0001013. D, Distribution of GC cells in G1, S and G2 phases assessed by flow cytometry. E, Detection of apoptosis in GC cells by flow cytometry. F, Colony formation experiment. G, The viability of HGC-27 cells was determined by CCK-8 assay. H, EdU experiment to detect cell proliferation. I, Cell migration measured by scratch test. J, Cell invasion evaluated by Transwell assay. \*  $p < 0.05$  vs. the NC group. Each experiment was repeated three times.

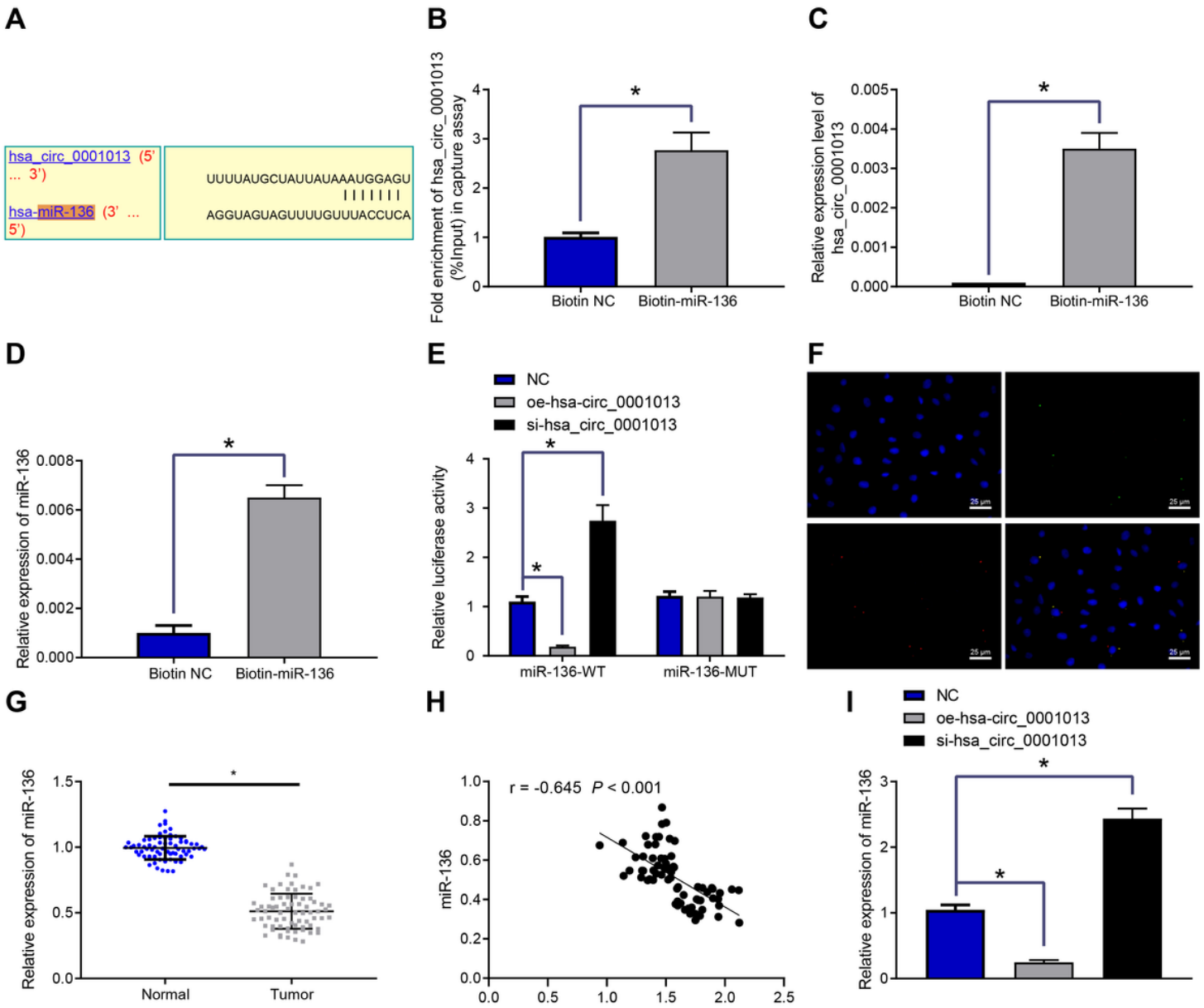


**Figure 3**

hsa\_circ\_0001013 binds to miR-136 in GC cells. A, Targeted binding of circ\_0001013 to miR-136. B, RT-qPCR to detect hsa\_circ\_0001013 captured by bio-coupled miR-136. C, hsa\_circ\_0001013 enriched by specific probe detected by RT-qPCR. D, Enrichment of miR-136 by hsa\_circ\_0001013 specific probe detected by RT-qPCR. E, Dual-luciferase reporter assay to verify binding relationship between circ\_0001013 and miR-136. F, Co-localization of hsa\_circ\_0001013 and miR-136 detected by FISH ( $\times 400$ ). G, RT-qPCR to estimate the expression of miR-136 in GC and adjacent tissues. H, Correlation analysis of hsa\_circ\_0001013 and miR-136 expression in GC tissues. I, Expression of miR-136 in MGC-803 cells after silencing or overexpressing hsa\_circ\_0001013. \*  $p < 0.05$ . Each experiment was repeated three times.

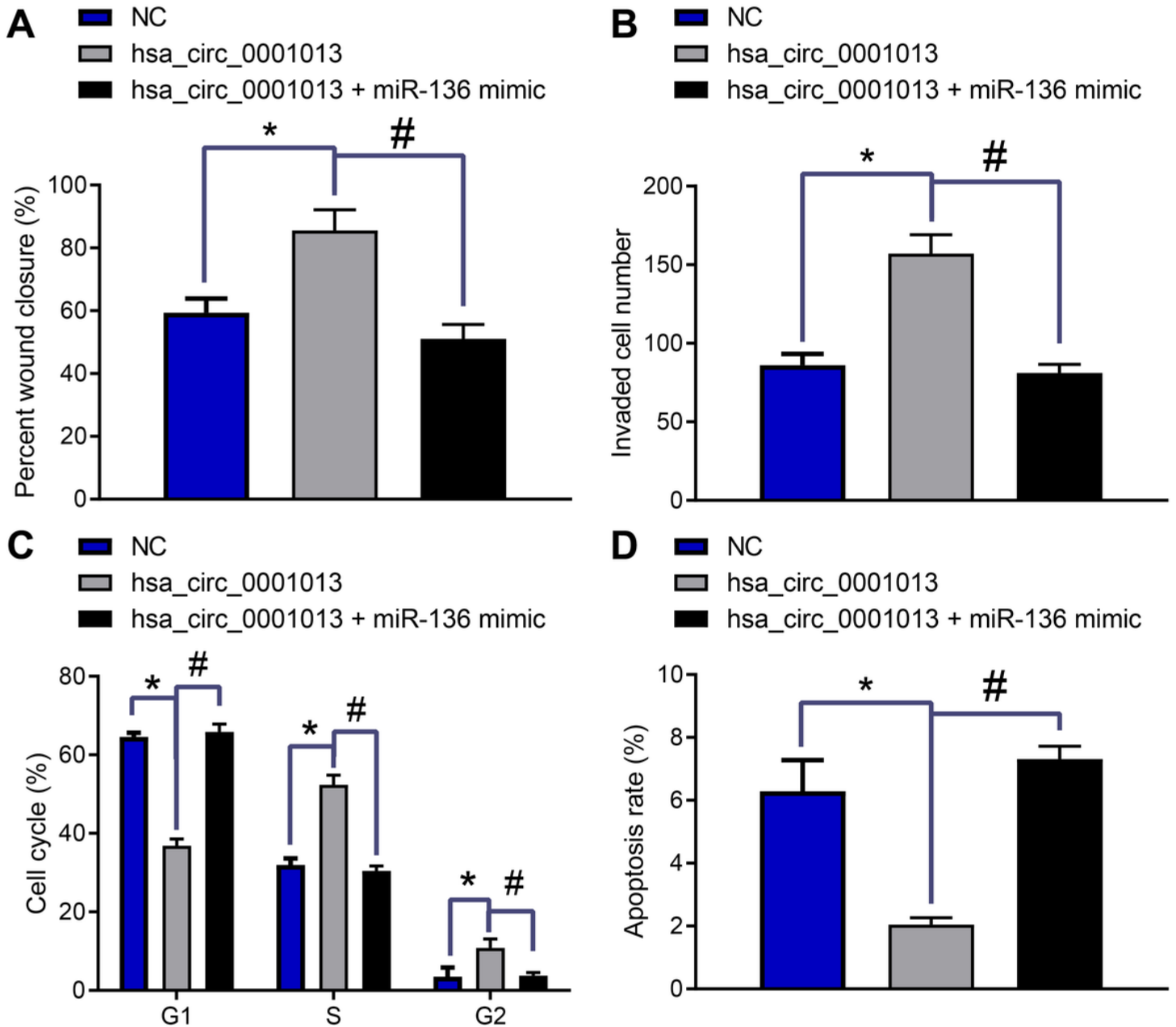


**Figure 4**

miR-136 inhibits the migration and invasion of GC cells to counteract the cancer promoting effect of hsa\_circ\_0001013. MGC-803 cells were transfected with NC, hsa\_circ\_0001013, or hsa\_circ\_0001013 + miR-136 mimic. A, Cell migration measured by scratch test. B, Invasion ability of GC cells determined by Transwell assay. C, Detection of GC cell cycle by flow cytometry. D, Apoptosis in GC cells measured by flow cytometry. \*  $p < 0.05$ . #  $p < 0.05$ . The experiment was repeated three times.

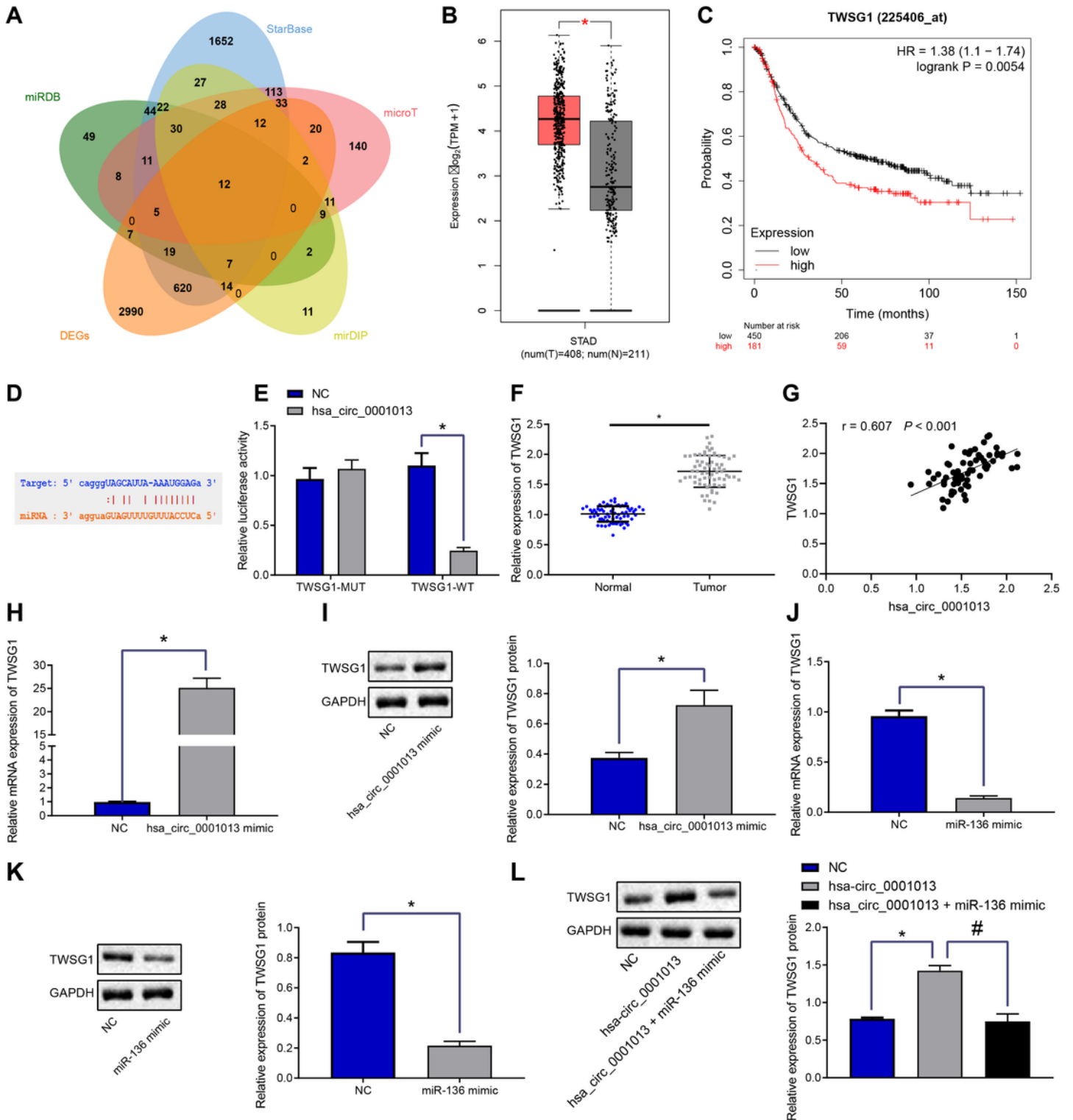


**Figure 5**

hsa\_circ\_0001013 causes TWSG1 upregulation by binding to miR-136. A, Venn map of intersection between target genes of miR-136 predicted by miRDB, StarBase, microT, and mirDIP and upregulated genes in GC. B, Expression of TWSG1 in GC in TCGA database. C, Survival curve of TWSG1 in GC. D, The binding sites of miR-136 and TWSG1 predicted by StarBase database. E, Targeting relationship between miR-136 and TWSG1 verified by dual-luciferase reporter assay. F, The expression of TWSG1 in GC tissues

and adjacent normal tissues detected by RT-qPCR. G, Correlation analysis of hsa\_circ\_0001013 and TWSG1 expression in GC tissues. H, RT-qPCR to detect the mRNA expression of TWSG1 after overexpressing hsa\_circ\_0001013. I, Western blot analysis to check the protein expression of TWSG1 after overexpressing hsa\_circ\_0001013 mimic. J, The mRNA expression of TWSG1 after miR-136 mimic treatment determined by RT-qPCR. K, Western blot analysis of the protein expression of TWSG1 after miR-136 mimic treatment. L, The protein expression of TWSG1 after co-transformation of hsa\_circ\_0001013 and miR-136 mimic detected by western blot analysis. \*  $p < 0.05$ . #  $p < 0.05$ . The experiment was repeated three times.

**Figure 6**

Low hsa\_circ\_0001013 expression inhibits xenograft tumor formation in nude mice. A, Tumor volume in mice. B, Tumor weight in mice. C, The expressions of TWSG1, Ki-67, MMP9 and CD34 in nude mice tested by western blot analysis. D, The expressions of TWSG1, Ki-67, MMP9 and CD34 in nude mice assessed by immunohistochemistry. \*  $p < 0.05$  vs. the NC group. The experiment was repeated three times.

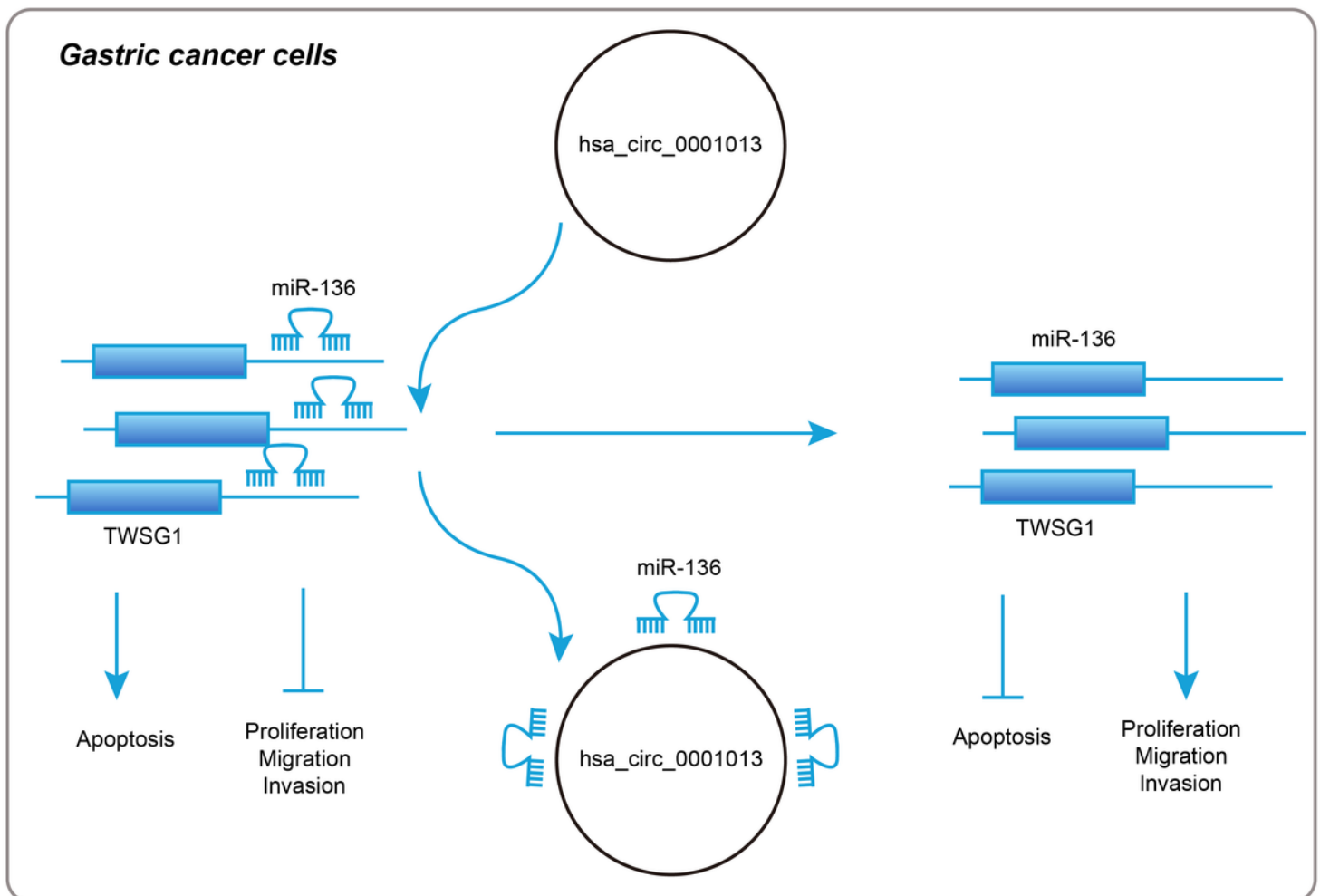


**Figure 7**

Mechanism. In GC cells, hsa\_circ\_0001013 bound to miR-136 which negatively targeted TWSG1. High expression of hsa\_circ\_0001013 decreased miR-136 expression to upregulate TWSG1, which promoted the proliferation, migration and invasion and inhibited the apoptosis of GC cells.